News from the Muon (g-2) Experiment at BNL

M. Deile[11] for the Muon (g-2) Collaboration:
G.W. Bennett[2], B. Bousquet[9], H.N. Brown[2], G. Bunce[2], R.M. Carey[1], P. Cushman[9], G.T. Danby[2], P.T. Debevec[7], M. Deile[11], H. Deng[11], W. Deninger[7], S.K. Dhawan[11], V.P. Druzhinin[3], L. Duong[9], E. Efstathiadis[1], F.J.M. Farley[11], G.V. Fedotovich[3], S. Giron[9], F. Gray[7], D. Grigoriev[3], M. Große-Perdekamp[11], A. Großmann[6], M.F. Hare[1], D.W. Hertzog[7], X. Huang[1], V.W. Hughes[11], M. Iwasaki[10], K. Jungmann[5], D. Kawall[11], B.I. Khazin[3], J. Kindem[9], F. Krienen[1], I. Kronkvist[9], A. Lam[1], R. Larsen[2], Y.Y. Lee[2], I. Logashenko[1], R. McNabb[9], W. Meng[2], J. Mi[2], J.P. Miller[1], W.M. Morse[2], D. Nikas[2], C. Onderwater[7], Y. Orlov[4], C.S. Özben[2], J. Paley[1], Q. Peng[2], C. Polly[7], J. Pretz[11], R. Prigl[2], G. zu Putlitz[6], T. Qian[9], S.I. Redin[3,11], O. Rind[1], B.L. Roberts[1], N.M. Ryskulov[3], Y.K. Semertzidis[2], P. Shagin[9], Yu.M. Shatunov[3], E. Sichtermann[11], E. Solodov[3], M. Sossong[7], A. Steinmetz[11], L.R. Sulak[1], A. Trofimov[1], D. Urner[7], P. von Walter[6], D. Warburton[2], A. Yamamoto[8].

[1] *Boston University, Boston, Massachusetts 02215, USA.*

[2] *Brookhaven National Laboratory, Physics Dept., Upton, NY 11973, USA.*

[3] *Budker Institute of Nuclear Physics, Novosibirsk, Russia.*

[4] *Newman Laboratory, Cornell University, Ithaca, NY 14853, USA.*

[5] *Kernfysisch Versneller Instituut, Rijksuniversiteit Groningen, 9747 AA Groningen, The Netherlands.*

[6] *Physikalisches Institut der Universität Heidelberg, 69120 Heidelberg, Germany.*

[7] *University of Illinois, Physics Dept., Urbana-Champaign, IL 61801, USA.*

[8] *KEK, High Energy Accelerator Research Organization, Tsukuba, Ibaraki 305-0801, Japan.*

[9] *University of Minnesota, Physics Dept., Minneapolis, MN 55455, USA.*

[10] *Tokyo Institute of Technology, Tokyo, Japan.*

[11] *Yale University, Physics Dept., New Haven, CT 06520,USA.*

The magnetic moment anomaly $a_\mu = (g_\mu - 2)/2$ of the positive muon has been measured at the Brookhaven Alternating Gradient Synchrotron with an uncertainty of 0.7 ppm. The new result, based on data taken in 2000, agrees well with previous measurements. Standard Model evaluations currently differ from the experimental result by 1.6 to 3.0 standard deviations.

1. Introduction

According to Dirac's theory, the gyromagnetic ratio g of a lepton is exactly 2. Deviations from this prediction are caused by radiative corrections to the lepton-photon vertex due to quantum field fluctuations. The anomaly of the electron is currently known at the level of 4 ppb [1] and well in agreement with the Standard Model. Since the contribution of heavy virtual particles to the anomaly $a = (g - 2)/2$ is proportional to the square of the mass scale, the sensitivity of the muon is enhanced by a factor $(m_\mu/m_e)^2 \approx 40000$ relative to the electron. At the present level of precision, the muon anomaly a_μ probes QED, weak and hadronic contributions.

2. Experimental Setup and Data Analysis

The general technique of the experiment at BNL is the same as that of the precursor experiment at CERN [2]. Polarised muons are stored in a highly uniform magnetic dipole field with electrostatic quadrupoles [3] providing vertical focussing. The muon spin precesses relative to the momentum vector with the angular frequency

$$\vec{\omega}_a = -\frac{e}{m_\mu} \left[a_\mu \vec{B} - \left(a_\mu - \frac{1}{\gamma_\mu^2 - 1} \right) \vec{\beta} \times \vec{E} \right], \quad (1)$$

provided that $\vec{\beta} \cdot \vec{B} = 0$. The dependence of ω_a on the electric field $\vec{E}$ (second term in Eq. (1)) is eliminated by storing the muons at the "magic" $\gamma_\mu = 29.3$, corresponding to a momentum $p_\mu =$

3.094 GeV/c. In this case, a_μ is given by simultaneous measurement of ω_a and $\langle B \rangle$, the magnetic field averaged over the spatial muon distribution in the storage region. As explained later, ω_a is reflected by the rate of decay positrons above a certain energy threshold. The magnetic field B is measured in terms of the free proton precession frequency ω_p in this field using nuclear magnetic resonance (NMR) probes. Then, a_μ can be expressed as

$$a_\mu = \frac{\omega_a/\omega_\mathrm{p}}{\mu_\mu/\mu_\mathrm{p} - \omega_a/\omega_\mathrm{p}} \,, \qquad (2)$$

where $\mu_\mu/\mu_\mathrm{p} = (318\,334\,539 \pm 10) \times 10^{-8}$ is the ratio of the magnetic moments of the muon to the proton, which has been measured with a precision of 30 ppb [4]. To avoid experimenter biases, a "blind analysis" strategy is pursued, separating the ω_a and ω_p analyses with secret offsets which are only revealed when both analyses are complete and internally consistent.

The beam used for the experiment originates at the Alternating Gradient Synchrotron (AGS) which every 2.5 s delivers 40–60 × 10^{12} protons at 24 GeV/c onto a nickel target. Each proton spill is composed of 12 bunches with a width of about 50 ns and a separation of 33 ms. Downstream of the target, pions at 3.1 GeV/c are selected into a 72 m long straight beam line where about half of them decay into muons. Because of parity violation in the pion decay, the selection of forward-going muons leads to a polarisation of about 96 %. Muons at the magic momentum are selected and injected into the storage ring through a hole in the yoke of the dipole magnet whose 1.45 T field is locally cancelled by a DC super-conducting inflector magnet [5]. To move the muons onto the central orbit, a kick of about 11 mrad is given by a pulsed kicker magnet [6]. The continuous superferric 'C'-shaped storage ring magnet [7] is excited by superconducting coils. The muon storage region has a 9 cm diameter cross-section and a central radius of 7.112 m, corresponding to a cyclotron period of 149.2 ns for muons at $\gamma = 29.3$.

A vertical air gap between pole and yoke decouples the yoke and pole pieces, which are fabricated from high quality steel, and allows the insertion of iron wedges to improve the field homogeneity by compensating the quadrupole field components. The four edge shims, 5 cm wide and about 3 mm high, are the main tool for reducing field variations over the beam cross-section. Surface coils glued to the pole pieces are used to further reduce the inhomogeneity of the field.

The field inside the storage region is mapped twice a week using a hermetically sealed cable-car with a matrix of 17 NMR probes moving on rails in the vacuum beam pipe and measuring a transverse field map about every 5 mm. The probes in the trolley are calibrated in place relative to a standard H_2O probe for which the calibration ratio $\omega_p(H_2O)/\omega_p(\text{free})$ between the precession frequencies of protons bound in water and free protons is known to 50 ppb [8].

During data taking, an array of 375 NMR probes embedded in the top and bottom plates of the vacuum chamber is used to monitor magnetic field variations between trolley measurements and to stabilise the field with a feed-back loop to the main magnet power supply [9].

Two independent analyses determined $\langle \omega_p \rangle$, averaged over the muon distribution. Their results agree within 0.05 ppm. The systematic uncertainties for $\langle \omega_p \rangle$ are summarised in Table 1. As a final result, the value $\langle \omega_p \rangle/(2\pi) = 61\,791\,595(00)(15)\,\text{Hz}$ (0.2 ppm) was obtained. The improvement from 0.4 ppm systematic error in 1999 to 0.24 ppm in 2000 comes mainly from the better field homogeneity (Figure 1) which was achieved by replacing the old inflector whose super-conducting fringe-field shield had a flux leak.

The decay positrons from $\mu^+ \rightarrow e^+ \nu_e \bar{\nu}_\mu$ range in energy from 0 to 3.1 GeV, and are detected with 24 lead/scintillating-fiber calorimeters [10] placed symmetrically around the inside of the storage ring. The arrival times and energies of the positrons are determined from the calorimeter pulses whose full shapes are sampled by a 400 MHz waveform digitiser (WFD). A laser and light-emitting-diode (LED) system is used to monitor potential time and gain shifts.

Because of parity violation in the weak muon decay, in the muon rest frame positrons are preferentially emitted along the muon spin direction. Since in the lab frame forward positrons
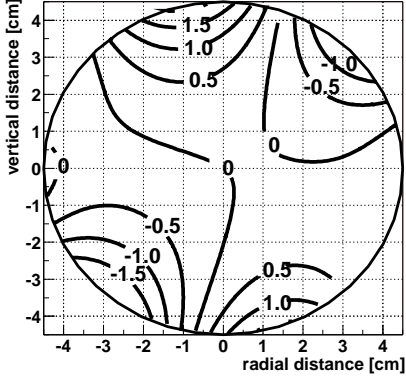
Figure 1. Magnetic field map of the storage ring cross-section averaged over azimuth. The contour lines have a distance of 0.5 ppm.

Table 1
Systematic uncertainties for the ω_p analysis.

Source of errors	Size [ppm]
Absolute calibration of standard probe	0.05
Calibration of trolley probes	0.15
Trolley measurements of central azimuthal average field	0.10
Interpolation with fixed probes	0.10
Uncertainty from muon distribution	0.03
Others[†]	0.10
Total systematic error on ω_p	0.24

[†] higher multipoles, trolley temperature and voltage response, eddy currents from kickers, and time-varying stray fields.

are boosted to high energies, the muon spin precession frequency modulates the decay positron count rate $N(t)$ if a lower energy threshold is applied:

$$N(t) = N_0\, e^{-\frac{t}{\gamma\tau}} \left[1 + A\cos\left(\omega_a t + \phi_a\right)\right]\ , \qquad (3)$$

where $\gamma\tau = 64.4\,\mu s$ is the dilated muon lifetime. For an energy threshold of 2 GeV, the asymmetry A is about 0.4. Figure 2 shows the sum of the decay positron time spectra observed by all detectors within a time range of $805\,\mu s$ or roughly 12 muon lifetimes. The total number of positrons recorded later than $45\,\mu s$ after injection is about 4×10^9. Error bars are drawn on all points but are only visible at very late times because of the

huge statistics of up to 10^7 entries per 149 ns time bin. Given this high number of events, the simple parametrisation in Eq. (3) proved not to be adequate for fitting the spectrum which is affected by several significant perturbations.
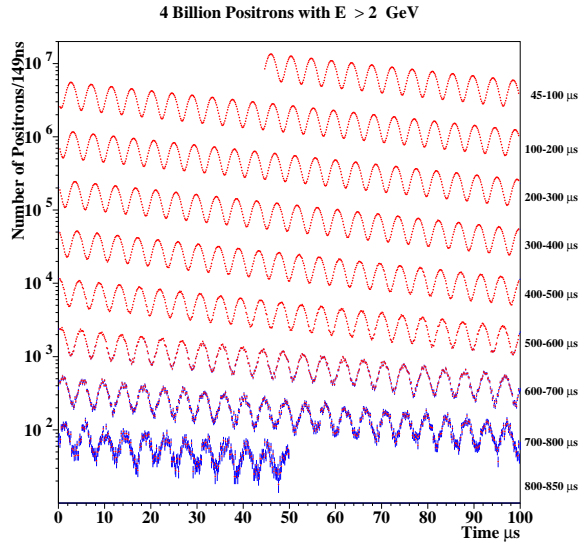

Figure 2. Positron time spectrum from the 2000 data set with all detectors combined.

We shall concentrate here on the leading systematic effect caused by coherent betatron oscillations – oscillations of the beam as a whole. Since the inflector aperture is smaller than the storage ring aperture, the phase space for betatron oscillations is not filled, which leads to a radial modulation of beam width and centroid. Looking from fixed detector positions, these oscillations have a frequency of 466 kHz, approximately given by $f_{\text{CBO}} \approx (1 - \sqrt{1-n})f_c$ where $f_c = 6.7\,\text{MHz}$ is the cyclotron frequency and $n = 0.136$ is the field index adjusted by the electric quadrupole voltage [3]. The value of n was chosen far away from physical resonance conditions which could lead to increased muon losses or spin flips. Since both the calorimeter acceptance and the energy distribution of the detected positrons depend on the radial position of the muon decay, the parameters N_0, A and ϕ_a in Eq. (3) receive a time modulation, e.g. $N_0(t) = N_0[1 + g_N(t)\cos(2\pi f_{\text{CBO}}t +$

ϕ_{CBO})], where $g_N(t)$ describes the CBO decay due to the muon momentum spread and higher $\vec{E}$ and $\vec{B}$ field multipoles. The time constant is typically $100\,\mu$s. The modulation $N_0(t)$ – with $g_N(0) \approx 1\%$ – was already observed and included in the analysis of the 1999 data set. Its parameters do not correlate strongly with ω_a. The modulations $A(t)$ and $\phi_a(t)$ are smaller – 0.1% and $1\,\mathrm{mrad}$ at $t = 0$ respectively – and were only discovered with the higher statistics of the 2000 data set. Their dangerous effect on the time spectrum is the creation of interference terms with the frequency $f_{\mathrm{CBO}} - \omega_a/(2\pi)$ which for our choice of n is very close to ω_a. This parametric resonance can produce shifts in ω_a of up to $4\,\mathrm{ppm}$ if individual detector time spectra are fitted without including $A(t)$ and $\phi_a(t)$. In the sum of all detector spectra, the shifts largely cancel thanks to the circular symmetry of the (g-2) ring. Remaining effects are accounted for by including $A(t)$ into the fit and assigning a systematic error for the impact of $\phi_a(t)$. Including $\phi_a(t)$ into the fit turned out to be more difficult because this term induces strong correlations between detector gain changes and ω_a, entailing further shifts in ω_a.

Other perturbations were treated like in earlier data sets [11]. Pulse pileup effects were removed by statistically superimposing recorded pulses from the data themselves and thus constructing an artificial pileup spectrum which was then subtracted from the untreated spectrum. The effects of beam debunching were eliminated by randomizing the start time of each fill over one cyclotron period. Muon losses were taken into account by multiplying the function in Eq. (3) with an extra loss term. AGS background due to erroneous proton extraction during the muon storage period, which contributed $0.1\,\mathrm{ppm}$ uncertainty to the 1999 result, was largely eliminated by installing a sweeper magnet in the beam line.

Four independent ω_a analyses with different approaches to take systematic effects into account were completed. Their results agreed within $0.4\,\mathrm{ppm}$ – as compared to statistically allowed variations of $0.5\,\mathrm{ppm}$ – and were combined to $\omega_a/(2\pi) = 229\,074.11(14)(7)\,\mathrm{Hz}$ ($0.7\,\mathrm{ppm}$). This number contains a correction of $+0.76(3)\,\mathrm{ppm}$ for residual effects of the electric field on muons with $\gamma \neq 29.3$ and for deviations from Eq. (1) due to vertical beam oscillations (i.e. $\vec{\beta} \cdot \vec{B} \neq 0$). The combined systematic errors listed in Table 2 account for the correlations between the results from the individual analyses.

Table 2
Systematic uncertainties for the ω_a analysis.

Source of errors	Size [ppm]
Coherent betatron oscillations	0.21
Pileup	0.13
Detector gain changes	0.13
Lost muons	0.10
Binning and fitting procedure	0.06
Others[†]	0.06
Total systematic error on ω_a	0.31

[†] AGS background, timing shifts, E field and vertical oscillations, beam debunching and randomisation.

3. Result from the Data Set of 2000 and Comparison with Theory

After completion of the ω_a and ω_p analyses, a_μ was calculated according to Eq. (2). The result is $a_{\mu^+} = 11\,659\,204\,(7)(5) \times 10^{-10}$ ($0.7\,\mathrm{ppm}$) [12]. It agrees well with older measurements (Figure 3). The new experimental world average, $a_{\mu^+} = 11\,659\,203\,(8) \times 10^{-10}$ ($0.7\,\mathrm{ppm}$), is dominated by the new result which has about half the uncertainty of previous measurements.

The Standard Model prediction for a_μ [14] can be written as

$$a_\mu(\mathrm{SM}) = a_\mu(\mathrm{QED}) + a_\mu(\mathrm{weak}) + a_\mu(\mathrm{hadronic}) \quad (4)$$

with $a_\mu(\mathrm{QED}) = 11\,658\,470.57(0.29) \times 10^{-10}$ and $a_\mu(\mathrm{weak}) = 15.1(0.4) \times 10^{-10}$. The hadronic contribution cannot be calculated from first principles at this time because it is dominated by low-energy interactions. The first-order hadronic vacuum polarisation contribution, $a_\mu(\mathrm{had}, 1)$, can be determined from measured e^+e^- annihilation cross-sections over all energies using a dispersion relation. It can also be related to hadronic τ decay. These calculations are still under theoretical investigation. Higher-order contributions are given by $a_\mu(\mathrm{had}, 2) = -10.0(0.6) \times 10^{-10}$ and $a_\mu(\mathrm{had, light-by-light}) = +8.6(3.2) \times 10^{-10}$.
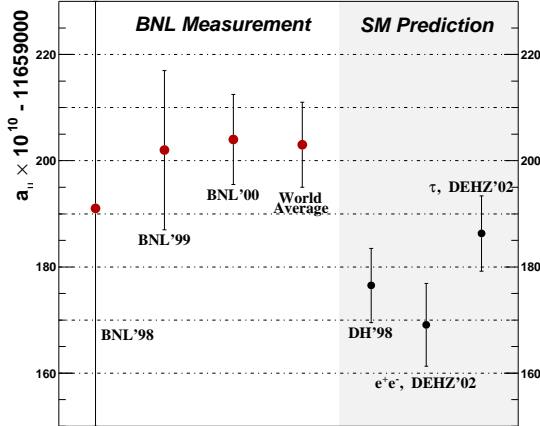
Figure 3. Recent experimental and theoretical values of a_μ. The labels for the theoretical predictions represent the evaluation of $a_\mu(\text{had}, 1)$ (see text).

For the latter, a sign error was recently corrected. Figure 3 shows the theoretical predictions for a_μ using recent evaluations of $a_\mu(\text{had}, 1)$. DH'98 [13] is the value used for the comparison in our PRL [12]. In this evaluation, $a_\mu(\text{had}, 1)$ uses data from both e^+e^- annihilation and τ decay. Later, new e^+e^- data from Novosibirsk [15] gave rise to a new calculation of $a_\mu(\text{had}, 1)$ which does not agree any more with the value obtained from τ decay data (DEHZ'02: [14]). Using the e^+e^--based result, $a_\mu(\text{had}, 1) = 684.7(7.0) \times 10^{-10}$, one obtains a total theory prediction $a_\mu(\text{SM}) = 11\,659\,169.1\,(7.8) \times 10^{-10}$ (0.7 ppm). Using the τ-based result, $a_\mu(\text{had}, 1) = 701.9(6.1) \times 10^{-10}$, one obtains a total theory prediction $a_\mu(\text{SM}) = 11\,659\,186.3\,(7.1) \times 10^{-10}$ (0.6 ppm). The deviations of the two evaluations from the experimental result correspond to 3.0 and 1.6 standard deviations, respectively. Hence, no unambiguous statement about new physics can be made at present.

4. Outlook

In the year 2001, the experiment was performed with negative muons and with different field indices n moving the CBO frequency away from the parametric resonance. The resulting data set of about 3×10^9 electrons is currently being analysed. It will provide a test of CPT invariance and – if CPT holds – an improved combined value of $a_{\mu\pm}$. However, in order to achieve the design goal of 0.35 ppm statistical uncertainty, additional 6×10^9 events are needed. A new run is planned, but at present funding is uncertain.

REFERENCES

1. R.S. Van Dyck Jr., P.B. Schwinberg and H.D. Dehmelt, Phys. Rev. Lett. 59, 26 (1987).
2. J. Bailey et al., Nucl. Phys. B., Vol. B150, No. 1, pp. 1-75, 1979.
3. Y. Semertzidis et al., accepted for publication in Nucl. Instr. Meth. A.
4. W. Liu et al., Phys. Rev. Lett. 82 (1999) 711.
5. A. Yamamoto et al., Nucl. Instr. Methods A 497 (2002) 23-40.
6. E. Efstathiadis et al, accepted for publication in Nucl. Instr. Methods A.
7. G.D. Danby, et al., Nucl. Instr. Meth. A 457 (2001) 151.
8. X. Fei et al., Nucl. Instr. Meth. A. 394 (1997) 349.
9. R. Prigl et al., Nucl. Instr. Meth. A 374 (1996) 118.
10. S.A. Sedykh et al., Nucl. Instr. Meth. A 455, 346 (2000).
11. H.N. Brown et al., Phys. Rev. Lett. **86**, 2227 (2001).
12. G.W. Bennett et al., Phys. Rev. Lett. **89**, 101804 (2002).
13. M. Davier and A. Höcker, Phys. Lett. **B435**, 427 (1998).
14. M. Davier et al., hep-ph/0208177, and references therein.
15. R.R. Akhmetshin et al., Phys. Lett. **B527**, 161 (2002).